Analytical Methods

Accepted Manuscript

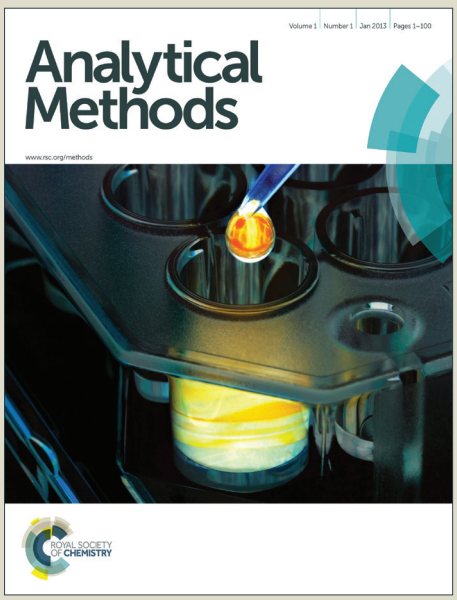

ROYAL SOCIETY OF CHEMISTRY

www.rsc.org/methods

A novel, fast and cost effective graphene - modified graphite pencil electrode for trace quantification of L-tyrosine

Nadeem Baig and Abdel-Nasser Kawde*

Chemistry Department, King Fahd University of Petroleum and Minerals, Dhahran, 31261, Saudi Arabia.

Tel: +966 3 860 2145

Fax: +966 3 860 4277

* Author for correspondence: E-mail: akawde@kfupm.edu.sa

A simple and novel method of detecting L-tyrosine in urine was introduced using a graphene-modified graphite pencil electrode (GR-modified GPE). Graphene oxide (GO) was directly reduced using cyclic voltammetry (CV) on the surface of the GPE. Synthesized GO was characterized by FTIR and Raman spectroscopy. The morphology of the electrode surface was characterized by field emission-scanning electron microscopy (FE-SEM) and the electrochemical properties were characterized by CV, electrochemical impedance spectroscopy (EIS), and square wave voltammetry (SWV). The graphene layer on the GPE dramatically enhanced the electroactive surface area and electrochemical oxidation of the L-tyrosine. A satisfactory linear response was obtained in the square wave voltammogram from 0.8 μM to 60 μM, with a regression constant (R^2) of 0.9995. The modified electrode yielded a low L-tyrosine limit of detection of 0.07 μM. The present modification process is completed within 5 min compared to other time-consuming reported methods. The modified electrode surface was free from interfering species, and successfully applied for the determination of the L-tyrosine in human urine. The low in cost and easy to modify electrode displayed excellent sensitivity, selectivity, reproducibility, a low limit of detection and a wide linear response range.

Keywords: Graphene, Graphite pencil electrode, L-Tyrosine, Human urine, Impedance spectroscopy, Square wave voltammetry, Sensor

1. Introduction

L-tyrosine is an essential amino acid with significant importance in the body. Its presence is crucial to regulating protein synthesis. L-tyrosine assists the maintenance of a positive nitrogen balance in the body[1]. Tyrosine is a precursor to several neurotransmitters, such as norepinephrine, dopamine, and epinephrine[2,3], and to hormones such as thyroxin, a critical thyroid hormone.[4] L-tyrosine is added to the foods, pharmaceuticals and dietary products.[5] The metabolic stability of the nicotinic acetylcholine receptor in the muscles is controlled by the phosphotyrosine level[6] Tyrosine is produced in the body by phenylalaninase from phenylalanine. The absence of this enzyme favors the production of phenylpyruvic acid, which can cause mental retardation[7] Sister chromatid exchange in the culture medium may increase at high concentrations of L-tyrosine.[8] The absence of tyrosine causes depression[9], and several investigations have reported that L-tyrosine is useful for treating fatigue, cold, stress, and wakefulness[10]. L-tyrosine is involved in several diseases such as alkaptonuria, albinism, mental illness, lung disease, liver disease, and tyrosinemia.[11] L-tyrosine excretion in the urine increased in patients suffering from diabetes mellitus.[12] The importance of L-tyrosine in the body has motivated a need to develop a sensitive, rapid, reproducible, and low cost detection method.

Several methods have been designed and reported for the determination of the L-tyrosine in biological samples and pharmaceutical products. These methods are mainly based on liquid chromatography tandem mass spectrometry[13,14], gas chromatography, chemiluminescence[15], high

performance liquid chromatography fluorescence or ultra violet (UV) detection[16–20] fluorimetry [21], and spectrophotometric and capillary electrophoresis.[22,23] Although all these methods display a good accuracy, most of them are tedious, require several preparatory steps prior to testing are time-consuming, and require a skilled practitioner. Electrochemical methods are advantageous in that they are low in cost, rapid, highly sensitive, selective, and provide good reproducibility.

Several previous reports have described electrochemical methods that are useful for determining L-tyrosine concentrations. A nafion-CeO_2 modified GCE[24], an iron(III) doped zeolite-CPE[25], and a AuNP-MWCNT-GCE[26] have been used for L-tyrosine detection in human blood, and a multi-wall carbon nanotubes GCE[7], a thiolated-β-cyclodextrins gold electrode[27] and a B-doped diamond electrode[28] have been used to detect L-tyrosine in a pharmaceutical product. A p-AMT GCE[29] has been tested for its utility in detecting L-tyrosine in human urine.

Carbon exits in several microstructural forms, such as glassy carbon, diamond, graphite, carbon fibers, carbon dots, graphene or nanotubes. Each form has its distinct attractive characteristics. Graphene is unique due to its excellent electrical conductivity[30], thermal and mechanical properties[31], and tremendously large surface area.[32] Graphene also provides a good mechanical strength, is low in cost[33], and is simple to produce in large scales.[34] These attractive features have led to the large-scale use of graphene in catalysis and to the development of electrochemical sensors.[32,35,36] On the other hand, the graphite pencil electrode has many advantageous over other carbon-based electrodes, due to its cost effectiveness, easy to handle and disposability.[37]

The objective of the present work is to develop a sensitive and convenient method for detecting L-tyrosine in biological samples. We report on the fabrication and characterization of a GR-

modified GPE. The modification of GPE compared to GCE, is rapid and simple. The electrochemical activity of the fabricated electrode increased markedly in the presence of L-tyrosine, in contrast with the corresponding activity of a bare GPE. To the best of our knowledge, this is the first example of L-tyrosine determination using a GR-modified GPE.

2. Materials and methods

2.1. Reagents

Tyrosine, L-methionine, ascorbic acid, fructose, potassium chloride and sodium chloride were supplied by Sigma-Aldrich (USA). Solutions of copper, nickel, zinc (1000 ppm), phenylalanine and alanine were received from Fluka (USA). Graphite was obtained from Fischer Science Education (USA). Double distilled water was used throughout the experiments and for solution preparation. The water was obtained directly from Water Still Aquatron A 4000 D (UK).

2.2. Apparatus

EIS, CV and SWV experiments were performed using an electrochemical work-station (Auto Lab, Netherland), coupled with a conventional three-electrode system. The working electrode was a GR-modified GPE or a bare GPE, the reference electrode was an Ag/AgCl (in 3 M KCl, CHI 111, CH instruments Inc.) and a platinum wire (CHI 115, CH instrument Inc.) was an auxiliary electrode. The GPE pencil mounted vertically such that 7mm of the pencil lead was outside the pencil holder and dipped in the measuring solution. The pencil electrode is already described in detail.[38] The three-electrode system was inserted through plastic Teflon into a 3 mL glass cell. All weights were measured using an electrical balance (GR-200). During the experiments, different pH buffers (5.5, 6.0, 6.7, 7.0, 7.5) were prepared, and the pH was controlled using a pH meter (accumet® XL50). Raman spectra was obtained by HORIBA

Scientific LabRAM HR Evolution (Japan). FE-SEM images were recorded using TESCAN LYRA 3 (Brno, Czech Republic) at the Center of Research Excellence in Nanotechnology, KFUPM.

2.3. Preparation of the GR-modified GPE

The GO (4 mg/mL) was dispersed in a 0.1 M acetate buffer at pH 4.8 and uniform dispersion was obtained by sonicating the solution for 2 hours. The GO solution was then transferred into 3 mL cell. The graphite pencil electrode and the Pt counter electrode and Ag/AgCl reference electrode were immersed into the GO solution. The GO was electrochemically reduced on the surface of the GPE under a cyclic sweeping potential from -1.4 V to +0.3 V applied at a scan rate of 20 mV/s over 2 cycles. As a control experiment, the graphite pencil electrode was electrochemically treated the same, yet in absence of GO to prepare the pretreated GPE. All experiments were conducted at room temperature.

3. Results and Discussion

3.1. Characterization and optimization of synthesized GO

GO was prepared by Hummers method. Synthesized GO was characterized by FTIR and Raman spectra (Fig. 1). The spectrum of GO (Fig. 1Ab) showed alkoxy –C-O stretching at 1050 cm^{-1}, epoxy –C-O stretching at 1225 cm^{-1}, carboxylic acid –C-O stretching at 1383 cm^{-1}, aromatic carbon double bond absorbance at 1625 cm^{-1}, carboxyl carbonyl absorbance at 1733 cm^{-1} and hydroxyl group stretching at 3425 cm^{-1}.[39] On the other hand, no prominent absorbance was observed for the graphite FTIR spectrum (Fig. 1Aa). The presence of these functional groups confirmed the formation of the GO from the graphite. The graphite Raman spectra (Fig. 1Ba) showed a weak D band at 1344 cm^{-1} and a strong prominent peak of G band at 1567 cm^{-1} which

is E2g first order scattering and 2D band was observed at 2693 cm^{-1}. In GO Raman spectra (Fig. 1Bb) a prominent D band appeared at 1350 cm^{-1} compared to the graphite D band. This is may be due to the extensive oxidation of the graphite which reduced the size of the in plane sp^2 domain. G band appeared at 1594 cm^{-1} and 2D band at 2670 $cm^{-}1$.[40] Id/Ig ratio was 0.98. The FTIR and Raman spectra confirmed the formation of GO from the graphite.

Synthesized GO was dispersed 10 mg/mL in 0.1 M acetate buffer by sonication for 2 hours. In order to enhance the sensitivity of the electrode, the GO concentration, scan numbers, scan window and scan rate were optimized for 1 mM L-tyrosine. The maximum response was obtained at 4 mg/mL GO over 2 CV cycles from -1.4 to +0.3 V at 0.02 V/s scan rate. Moreover, different electrolyte and technique were also scanned, and the best response observed with 0.1M PBS and SWV voltammetry (Table. 1).

3.2. Morphological and electrochemical characterization of the bare and GR- modified GPE

The surface morphologies of the bare and GR-modified GPEs were analyzed using the FE-SEM. Prior to analysis, the electrode was modified by directly reducing GO (4 mg/ mL) on the surface of the GPE over two CV scans from - 1.4 V to 0.3 V. The FE-SEM images were collected from the bare and the GR-modified GPEs at three different magnifications to optically image the surface (Figs. 2 A, B, and C). Figures 2-a and 2-b show the bare GPE and GR-modified GPE, respectively. A comparison of the bare 10 µm SEM image with the modified GPE clearly reveals the formation of the graphene layer on the GPE surface. Figure 2Ab (10 µm) reveals that a small uncovered region was present on the GPE whereas the rest of the GPE was covered by the graphene layer. High magnification images further revealed the structure of the nm thick wrinkled sheets of the graphene on the surface of the graphite pencil electrode (Fig. 2-Cb). The

wrinkled graphene sheet is extremely valuable for enhancing the surface area of the electrode because these wrinkled shapes are much more stable and do not easily revert to the graphitic form.[41]

EIS was used to investigate the electrochemical properties of the electrode. Electrochemical impedance spectra were recorded from a solution comprising 5 mM $K_3Fe(CN)_6/K_4Fe(CN)_6$ and 0.1 M KCl. The frequency range is varied from 100 kHz to 0.01 Hz. Figure 3 plots the electrochemical impedance properties of the GR-modified and the bare GPE. The Z and –Z axes indicate the real and negative values of the imaginary impedance variables, respectively. The semicircular part of the graph at high frequencies in the Nyquist plot indicates a limiting charge transfer process, whereas the straight line at low frequencies corresponds to a diffusion process. The charge transfer resistance (R_{CT}) was calculated directly from the semicircular Nyquist diagram. The R_{CT} values calculated from the impedance spectra were 2941 Ω and 29.68 Ω for bare and GR-modified GPE, respectively. The data revealed that graphene layer on the surface of the GPE significantly reduced the charge transfer resistance compared to the bare GPE (Fig. 3).

The electroactive surface area of the bare and GR-modified GPE could be calculated with the help of the Randles-Sevcik equation:

$$Ip = 2.69 \times 10^5 \, C \, n^{3/2} A \, D^{1/2} \gamma^{1/2}, \qquad 1$$

where C is the concentration of the analyte (mol L^{-1}), n is the number of electrons that contribute to the redox reaction on the electrode surface, A is the electroactive surface area of the electrode (cm^2), D is the diffusion coefficient (cm^2s^{-1}) and γ is the scan rate (Vs^{-1}). The electroactive surface area was calculated from the CV scans recorded between 20 mV and 300 mV using the GR-modified GPE or the bare GPE (Data not shown) from a solution comprising 5 mM

$K_3Fe(CN)_6/K_4Fe(CN)_6$ and 0.1 M KCl. The electroactive areas calculated using equation 1 was 0.592 cm^2 and 0.0501 cm^2 for the GR-modified GPE and the bare GPE, respectively.

The k electron transfer rate constants of the bare and the GR-modified GPE were calculated using equation 2. [42,43]

$$R_{CT} = R\ T / F^2\ n^2\ k\ A\ C,$$

$$k = R\ T / F^2\ n^2\ A\ C\ R_{CT}, \qquad 2$$

where R_{CT} is the charge transfer resistance, T is the temperature, R is the gas constant, F is the Faraday constant, n is the number of electron, A is the electroactive area of the electrode, and C is the concentration. The calculated electron transfer rate constants (k) of the bare and GR-modified GPE were 3.62×10^{-4} cm s^{-1} and 3.03×10^{-3} cm s^{-1}, respectively. The higher value of k for the GR-modified GPE indicated that the electron transfer process was much faster than the electron transfer rate constant at the bare GPE.

Further electrochemical studies were performed by collecting the CV and SWV curves in a tyrosine PBS buffer solution (0.1 M, pH 6.7). The oxidation peak current response at the surface of the GR-modified GPE in the 1 mM L-tyrosine solution (Fig. 4b) was increased dramatically as compared to the corresponding response on the bare GPE (Fig. 4a). Similar results were obtained using square wave voltammetry. The electrochemical responses in the presence of the 50 µM L-tyrosine solution were much stronger at the GR-modified GPE than at the bare GPE in a 0.1M PBS buffer (pH, 6.7) (Fig. 5). The current at the GR-modified GPE was 104 times the current measured at the bare GPE (Fig. 5). The graphene solution was prepared in a 0.1 M acetate buffer (pH 4.8), and it is possible that the acetate pretreatment may have affected the electrochemical properties of the GPE. This possibility was tested by the pretreating the bare GPE between - 1.4

and 0.3 V under the same set of conditions as the graphene reduced on the surface of the GPE, over 2 cycles. Figure 6b shows that only the 0.1 M acetate buffer did not affect the peak current in the presence of L-tyrosine. GO acts as an insulator rather than as a conductor, whereas in its reduced form, it is an excellent conductor.[31] The morphological and electrochemical results agreed well with one another, and the GO appeared to be successfully reduced on the GPE surface, yielding enhanced electroactivity, sensitivity, and an increase in the electroactive surface area compared to the bare GPE.

Effect of pH

The effect of the pH was examined using SWV in a PBS buffer (0.1 M) comprising 50 μM L-tyrosine at a pH ranging from 5.5 to 7.5 (Fig. 6). The pH affected the peak current of the L-tyrosine oxidation reaction. In addition to the current variations, the oxidation peak potential was observed to shift with the pH. The oxidation peak current increased as the pH increased and reached its maximum value at pH 6.7. Further increases in pH reduced the current (Fig. 6B). The peak position of the L-tyrosine oxidation reaction shifted linearly as the pH increased (Fig. 6B, inset). The negative shift in the oxidation potential of L-tyrosine established that protons were directly involved in its oxidation. The slope of a linear plot (R^2 = 0.9938) of the oxidation peak potential vs. pH (Fig. 6B, inset) was - 59.6 mV, near the theoretical value of - 59 mV. This slope indicated that equal numbers of protons and electrons were involved in the process of charge transfer on the surfaces of the GR-modified GPE (Eq. 3). The electrooxidation of tyrosine at the GR-modified GPE was a one-electron and one-proton process, in agreement with previous reports, and the reaction mechanism is shown in Scheme 1.[4,7,24,44]

$$E \text{ vs. } Ag/AgCl = 1.0356\text{-}0.0596[pH] \qquad 3$$

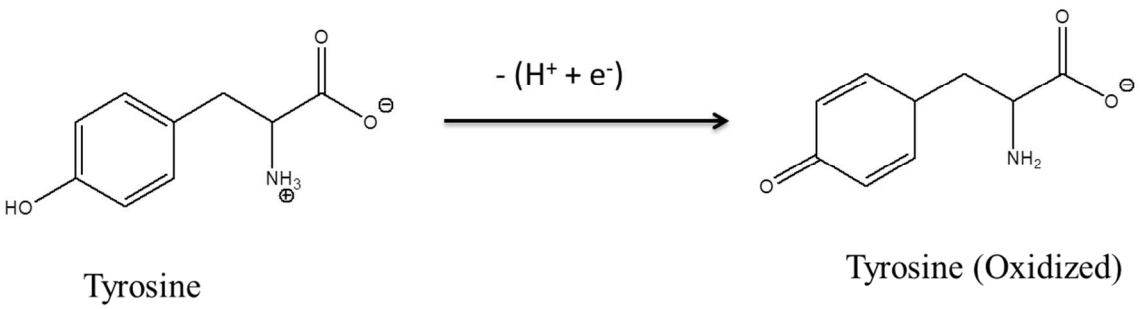

Scheme 1. The electrochemical mechanism of L-tyrosine oxidation.

3.3. Optimization of the SWV parameters

In an effort to develop a highly selective and sensitive electroanalytical method, we optimized each instrumental variable that could affect the L-tyrosine oxidation response under SWV measurements at a GR-modified GPE.

The amplitude of the square wave potential was first optimized between 0.02 V and 0.06 V as this parameter significantly impacted the oxidation signal of L-tyrosine. As the amplitude increased, the current also increased. A maximum current was obtained at 0.03 V above which the value decreased continuously (Data not shown). Next, the frequency was optimized between 25 and 80 Hz. The frequency affected the L-tyrosine oxidation signal strength. The highest current obtained at 50 Hz (Data not shown). Finally, the L-tyrosine adsorption time on the GR-modified GPE surface was optimized. The adsorption time significantly influenced the sensitivity and the strength of the signal. The oxidation peak current increased as the adsorption time increased. The increase in current indicated that L-tyrosine adsorbed onto the modified electrode surface. The electrode surface became saturated at 210 s, after which peak current became constant (Data not shown). The optimized square wave potential was characterized by amplitude of 0.03 V, a frequency of 50 Hz, and an adsorption time of 210 s.

3.4.Calibration curve and the detection limit

A calibration curve was constructed using the optimized square wave parameters, including amplitude of 0.03 V, frequency of 50 Hz, and the adsorption time of 210 s. The current and L-tyrosine concentration were linearly related between 0.8 μM and 60 μM (n = 3). A linear regression of the calibration curve yielded the equation: I (μA) = 12.441 C_{Tyr} (μM) - 1.8942, with a regression constant (R^2) of 0.9995 (Fig. 7). The detection limit obtained using the GR-modified GPE was 0.07 μM. The sensitivity and the lower detection limit of the modified electrode indicated that the electroactivity of the graphene on the GPE surface towards L-tyrosine was significantly enhanced. The limits of detection and quantification obtained at the GR-modified GPE are either comparable or even better than that obtained utilizing other modified electrodes already reported in literature (Table 2).

3.5.Reproducibility study

The reproducibility of the L-tyrosine detection properties was characterized by fabricating five GR-modified GPEs under the same set of conditions. Small deviations in the currents were observed using a 50 μM L-tyrosine solution in 0.1 M PBS (pH 6.7), with a relative standard deviation of 4.95% (n = 5). This small RSD value indicated the excellent reproducibility of the electrode developed here.

3.6. Applications and interference studies

The sensitivity of the L-tyrosine measurements to interference from other analyte was examined. Biomolecules such as phenylalanine, alanine, glucose, fructose, L-methionine, uric acid, ascorbic acid, and some common ions Na^+, K^+, Li^+, Ni^{+2}, SO_4^{-2} and Cl^{-1} were tested for their interference effects on the measurement. Most interference agents introduced small variations in the current, on the order of 0.3 - 12 %. This fabricated electrode was then tested in a real sample.

A urine sample was collected from a healthy person. Prior to analysis, the sample was diluted to 200 times in 0.1 M PBS buffer (pH 6.7). Urine samples spiked with 40, 50, or 60 μM L-tyrosine were measured under optimized conditions. The voltammograms yielded two well-defined peaks, one corresponding to uric acid and the other at +0.63 V corresponding to tyrosine. The signal recovered 89 to 95% at its initial value (Table 3). These results suggested that the GR-modified electrode may be useful for L-tyrosine detection in urine, which tends to include impurities and interfering species.

4. Conclusions

GO was reduced directly on the GPE surface using electrochemical method. The graphene layer on the GPE displayed enhanced electroactivity towards L-tyrosine, which provides a low the oxidation potential. The modified electrode provided an excellent linear response over the range 0.8 - 60 μM with a regression constant (R^2) of 0.9995. The enhanced signal of the L-tyrosine on the electrode indicated that graphene on the surface of the graphite pencil electrode significantly improved the electrode's conductivity and detection limit to 0.07 μM. Modification took around five minutes; hence, it is the fastest modification method among the so far reported ones. The presence of interfering species did not affect the sensitivity of the GR-modified GPE for L-tyrosine detection. The reproducibility studies indicated that the electrode fabrication process yielded a uniform clean electrode, which could be modified easily. The low cost, high selectivity, high sensitivity, low detection limit, and wide linear range indicate that this electrode provides a valuable tool for sensitive detection of L-tyrosine.

Acknowledgements

The authors would like to acknowledge the support received from King Fahd University of Petroleum and Minerals (KFUPM) through Project No. IN151010.

References

1 K. Huang, D. Luo, W. Xie, Y. Yu, Colloids Surf. B: Biointerfaces, 2008, **61,** 176–181.

2 J. Fernstrom, M. Fernstrom, J. Nutr., 2007, **137,** 1539S–1547S.

3 L. Jiang, S. Gu, Y. Ding, D. Ye, Z. Zhang, F. Zhang, Colloids Surf. B. Biointerfaces, 2013, **107,** 146–151.

4 Y. Fan, J. Liu, H. Lu, Q. Zhang, Microchim. Acta, 2011, **173,** 241–247.

5 R. Nie, X. Bo, H. Wang, L. Zeng, L. Guo, Electrochem. Commun., 2013, **27,** 112–115.

6 A Sava, I. Barisone, D. Mauro, G. Fumagalli, C. Sala, Neurosci. Lett., 2001, **313,** 37–40.

7 Q. Xu, S. Wang, Microchim. Acta, 2005, **151,** 47–52.

8 C. Li, Colloids Surf. B. Biointerfaces, 2006, **50,** 147–151.

9 M. Arvand, T. Gholizadeh, Colloids Surf. B. Biointerfaces, 2013, **103,** 84–93.

10 S. Hao, Y. Avraham, O. Bonne, E. Berry, Pharmacol. Biochem. Behav., 2001, **68,** 273–281.

11 G.Huang, J. Yang, Biosens. Bioelectron., 2005, **21,** 408–418.

12 G. Molnar, Z. Wagner, L. Marko, T. Koszegi, M Mohas, B Kocsis, Z Matus, L Wagner, M. Tamasko, I. Mazak, B. Laczy, J. Nagy, I. Wittmann, Kidney Int., 2005, **68,** 2281–2287.

13 N. Felitsyn, G. Henderson, M. James, P. Stacpoole, Clin. Chim. Acta, 2004, **350,** 219–230.

14 S. Bouchet, E. Chauzit, D. Ducint, N. Castaing, M. Raffin, N. Moore, K. Titier, M. Molimard, Clin. Chim. Acta, 2011, **412,** 1060–1067.

15 M. Alonso, L. Zamora, J. Calatayud, Talanta, 2003, **60,** 369–376.

16 M. Lee, H. Nohta, Y. Umegae, Y. Ohkura, J. Chromatogr., 1987, **415,** 289–296.

17 D. Machado, B. Willys, J. Cervantes, J. Chromatogr. B., 2008, **863,** 88–93.

18 M. Sa, L. Ying, T. Guo, X. Dong, R. Ping, Clin. Chim. Acta, 2012, **413,** 973–977.

19 G. Neurauter, S. Bürgi, A. Haara, S. Geisler, P. Mayersbach, H. Schennach, D. Fuchs, Clin. Biochem., 2013, **46,** 1848–1851.

20 X. Mo, Y. Li, A. Tang, Y. Ren, Clin. Biochem., 2013, **46,** 1074–1078.

21 N. Kiba, M. Ogi, M. Furusawa, Anal. Chim. Acta, 1989, **224**, 133–138.

22 C. Bayle, N. Siri, V. Poinsot, M. Treilhou, E. Caussé, F. Couderc, J. Chromatogr. A, 2003, **1013,** 123–130.

23 Y. Huang, X. Jiang, W. Wang, J. Duan, G. Chen, Talanta., 2006, **70,** 1157–1163.

24 A. Razavian, S. Ghoreishi, A. Esmaeily, M. Behpour, L. Monzon, J. Coey, Microchim. Acta., (2014).

25 A. Babaei, S. Mirzakhani, B. Khalilzadeh, J. Braz. Chem. Soc., 2009 **20,** 1862–1869.

26 T. Madrakian, E. Haghshenas, A. Afkhami, Sensors Actuators B Chem., 2014, **193,** 451–460.

27 C. Quintana, S. Suárez, L. Hernández, Sensors Actuators B Chem., 2010, **149,** 129–135.

28 G. Zhao, Y. Qi, Y. Tian, Electroanalysis 2006, **18,** 830–834.

29 S. Revin, S. John, Sensors Actuators B Chem., 2012, **161,** 1059–1066.

30 A. Geim, K. Novoselov, Nat. Mater., 2007, **6,** 183–191.

31 Y. Fang, E. Wang, Chem. Commun., 2013, **49,** 9526–9539.

32 K. Wang, Q. Liu, X. Wu, Q. Guan, H. Li, Talanta., 2010, **82,** 372–376.

33 H. Schniepp, J. Li, M. McAllister, H. Sai, M. Alonso, D. Adamson, R. Prudhomme, R. Car, D. Saville, I. Aksay, J. Phys. Chem. B., 2006, **110,** 8535–8539.

34 K. Wang, Q. Liu, Q. Guan, J. Wu, H. Li, J. Yan, Biosens. Bioelectron., 2011, **26,** 2252–2257.

35 N. Shang, P. Papakonstantinou, M. McMullan, M. Chu, A. Stamboulis, A. Potenza, S. Dhesi, H. Marchetto, Adv. Funct. Mater., 2008, **18,** 3506–3514.

36 Y. Wang,Y. Li, L. Tang, J. Lu, J. Li, Electrochem. Commun., 2009, **11,** 889–892.

37 M. Akanda, M. Sohail, M. Aziz, A. Kawde, Electroanalysis, 2015, **27**, 1-18.

38 M. Aziz, A. Kawde, Talanta, 2013, **115,** 214-221.

39 T. Yang, L. Liu, J. Liu, M. Chen, J. Wang J. Mater. Chem., 2012, **22,** 21909–21916.

40 S. Stankovich, D. Dikin, R. Piner, K. Kohlhaas, A. Kleinhammes, Y. Jia c, Y. Wu, S. T. Nguyen, R. Ruoff, Carbon, 2007, **45,** 1558–1565

41 P. Aneesh, S. Nambiar, T. Rao, A. Ajayaghosh, Anal. Methods, 2014, **6,** 5322-5330.

42 K. Ozoemena, Sensors, 2006, **6,** 874–891.

43 V. Ganesh, S. Pal, S. Kumar, V. Lakshminarayanan, J. Colloid Interface Sci., 2006, **296,** 195–203.

44 T. Madrakian, E. Haghshenas, A. Afkhami, Sensors and Actuators B, 2014, **193,** 451–460.

45 G. Jin, X. Lin, Electrochem. Commun., 2004, **6,** 454–460.

46 X. Tang, Y. Liu, H. Hou, T. You, Talanta, 2010, **80,** 2182–2186.

47 G. Jin, X. Peng, Q. Chen, Electroanalysis, 2008, **20,** 907–915.

48 M. Vasjari, A. Merkoçi, J. Hart, S. Alegret, Microchim. Acta., 2005, **150,** 233–238.

49 J. Okuno, K. Maehashi, K. Matsumoto, K. Kerman, Y. Takamura, E. Tamiya, Electrochem. Commun., 2007, **9,** 13–18.

Table 1 Optimization of the graphene oxide, electrolyte, and technique for 1mM L-tyrosine

Sr#	Parameter	Best Response	Analyzed Range
1	GO concentration	4 mg/mL	1-10 mg/mL
2	Scan number for GO reduction	2	1-7
3	Scan window for GO reduction	-1.4 V to 0.3 V	-1.6 – 0.6 V
4	Scan rate for graphene reduction	0.02 V/s	0.01 – 0.05 V/s
5	Electrolyte	0.1 M PBS	
6	Technique	SWV	

Table 2 Comparison of the GR-modified GPE properties to those of other modified electrodes for the determination of the L-tyrosine in a sample.

Electrode	LOD (µM)	Electrode Modification Time	Linear Range (µM)	Correlation coefficient	Ref.
Nafion-TiO_2-GR-GCE	2.3	C*	10-160	0.9941	4
Nafion-CeO_2-GCE	0.09	C*	2-160	0.9973	24
BuCh-GCE	0.4	65 min	4-100	-	45
CNF-CPE	0.1	C*	0.2-109	0.9985	46
MWNTs-GCE	0.4	12 hr	2-500	0.9967	7
Fe^{3+}/ZMCPE	0.32	24 hr	1.2-90	0.9989	25
B-doped diamond electrode	1	-	100-700	0.9972	28
MWCNTs-GNS/GCE	0.19	C*	0.90–95.4	0.9900	9
Ag/Rutin/WGE	0.07	100 min	0.3-10	0.9850	47
Screen Printed ES	-	-	50-500	0.9980	48
SWCNT arrayed-Pt	0.1	-	0.1-100	0.9996	49
Thiolated/β-cyclodextrins /gold electrode	12	6 hr	36-240	0.9970	27
GR-modified GPE	0.07	5 min	0.8-60	0.9995	This work

C*= Casting method is used and electrode dried at room temperature. Time is not mentioned

Table 3 Determination of L-tyrosine in human urine samples

Sr#	Added (µM)	Found (µM)	Recovery (%)
1	40	37.2	93
2	50	47.4	95
3	60	53.4	89

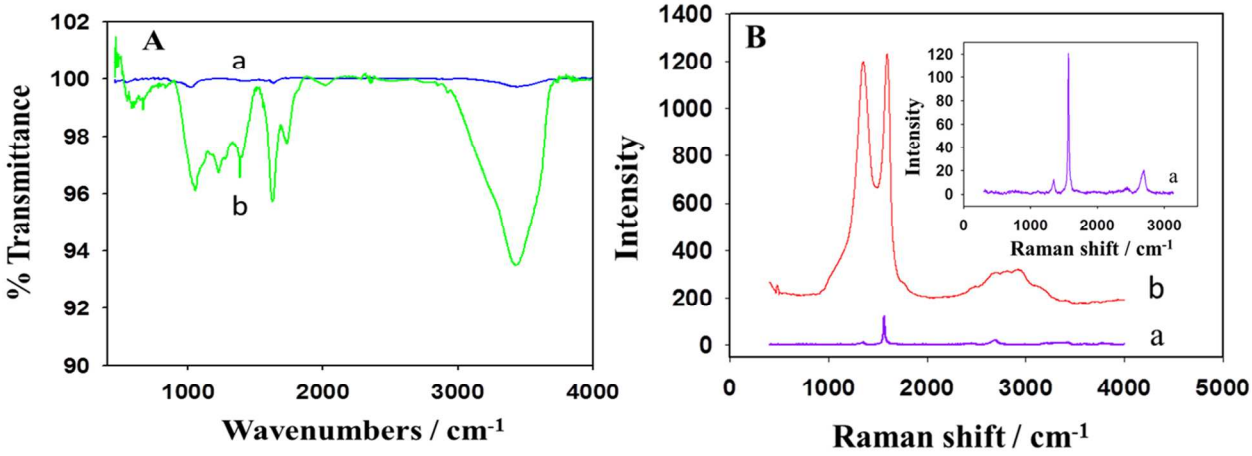

Fig. 1 (A) FTIR spectra of graphite (a) and GO (b), and (B) Raman spectra of graphite (a) and GO (b). Inset of B shows the graphite Raman spectrum.

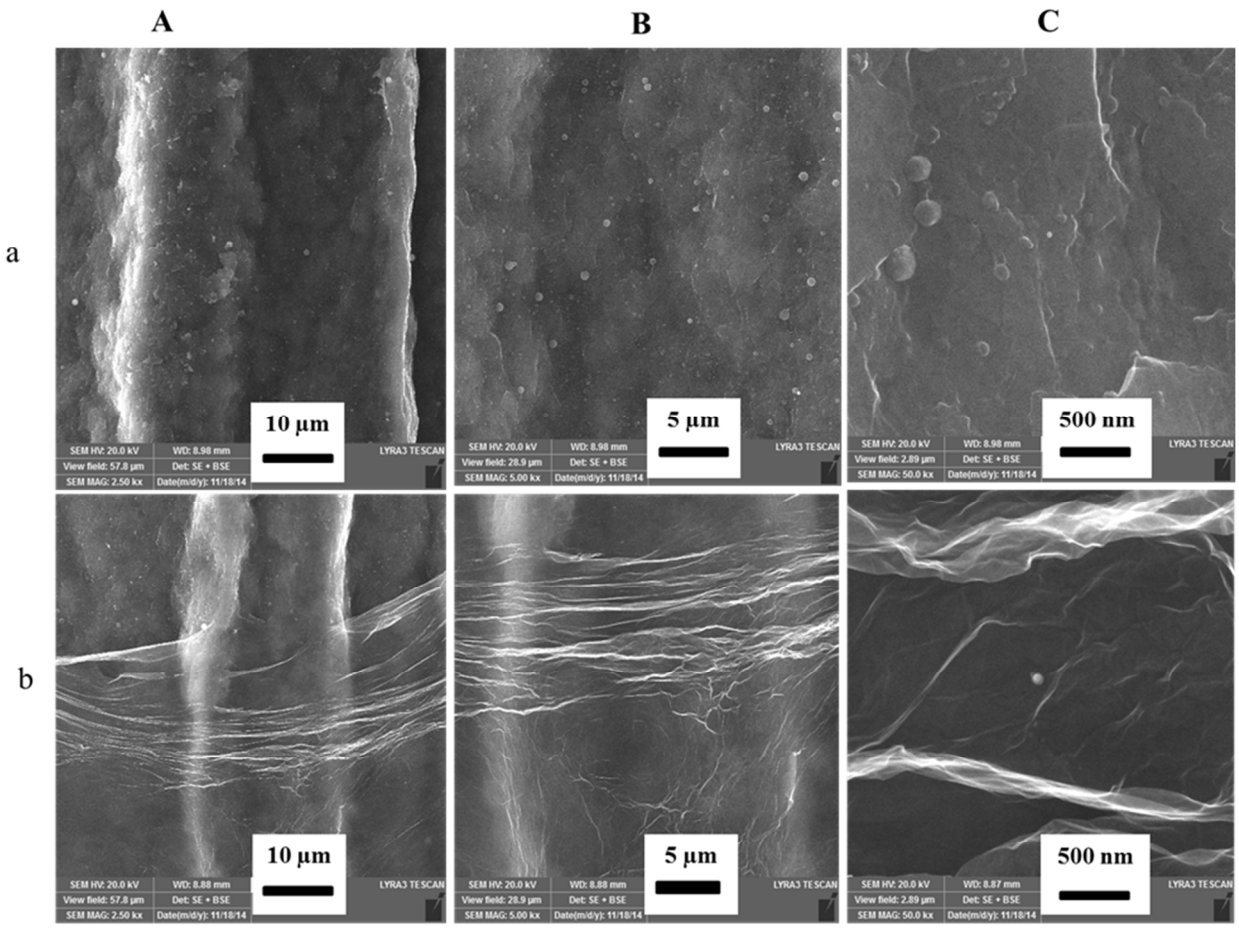

Fig. 2 FE-SEM images at three different magnifications: 10 µm (A), 5 µm (B), and 500 nm (C) of bare (a) or GR-modified GPE (b).

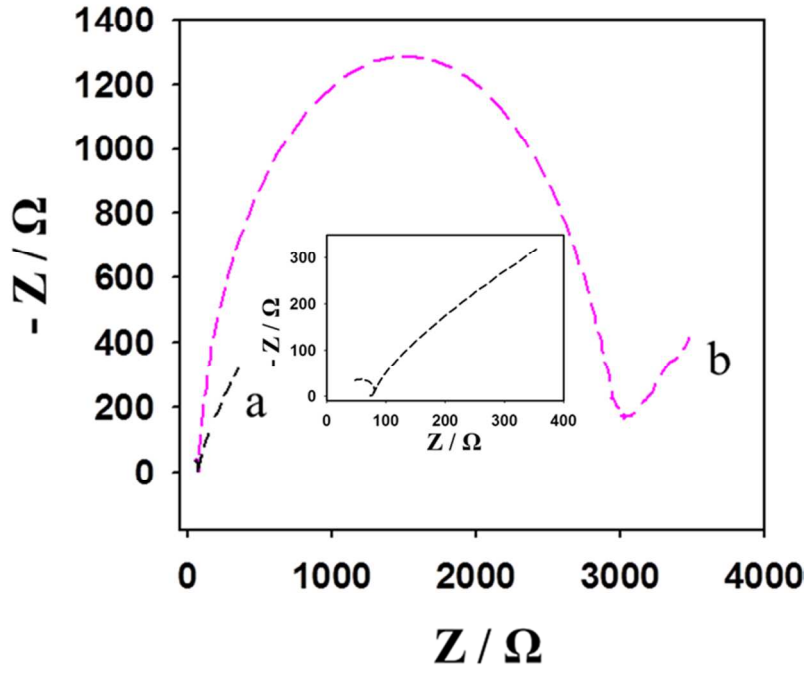

Fig. 3 (A) Electrochemical impedance spectra of the (a) GR-modified GPE, (b) bare GPE in a 0.1 M KCl solution containing 5 mM $K_3Fe(CN)_6/K_4Fe(CN)_6$ upon application of 50 mV potential in the frequency range 100 kHz to 0.01 Hz. Inset: Magnified impedance of the GR-modified GPE.

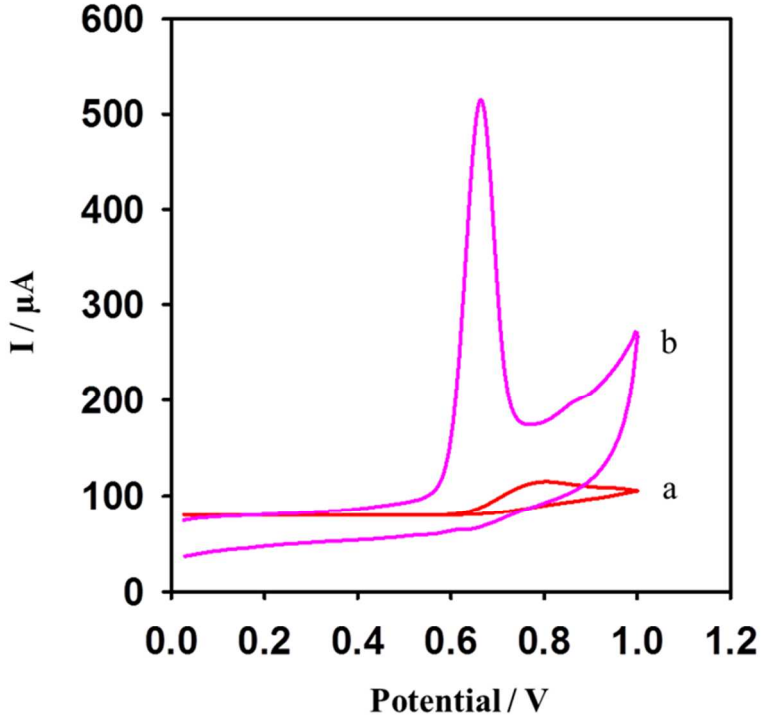

Fig. 4 Cyclic voltammograms of (a) the bare GPE, and (b) the GR-modified GPE in a 1 mM L-tyrosine PBS buffer (0.1 M, pH 6.7). Scan rate: 100 mV s^{-1}.

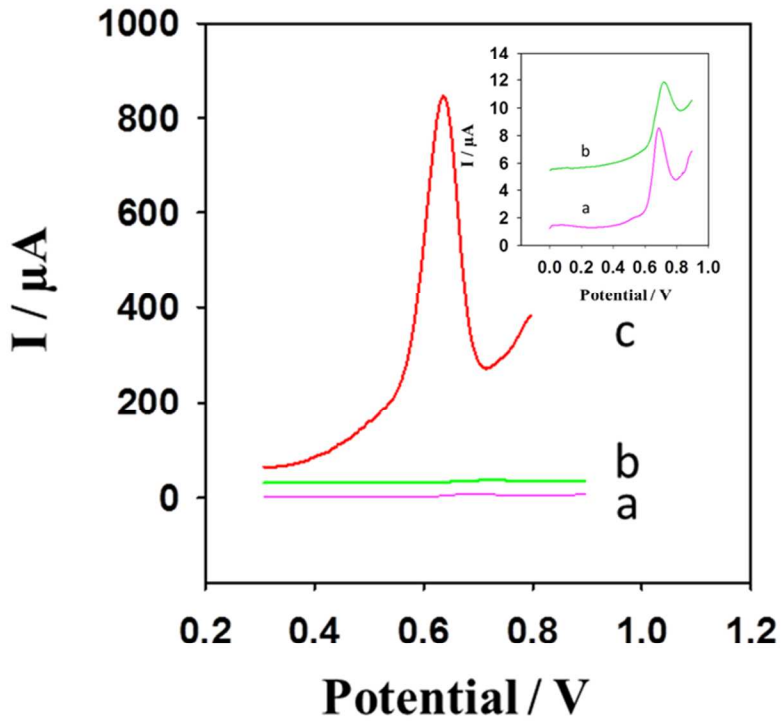

Fig. 5 Square wave voltammograms of 50 µM L-tyrosine in 0.1 M PBS (pH 6.7) on the (a) bare GPE, (b) pretreated GPE, and (c) GR-modified GPE. The parameters of the SWV experiment: amplitude 0.03 V, frequency 50 Hz, and adsorption time 210 s.

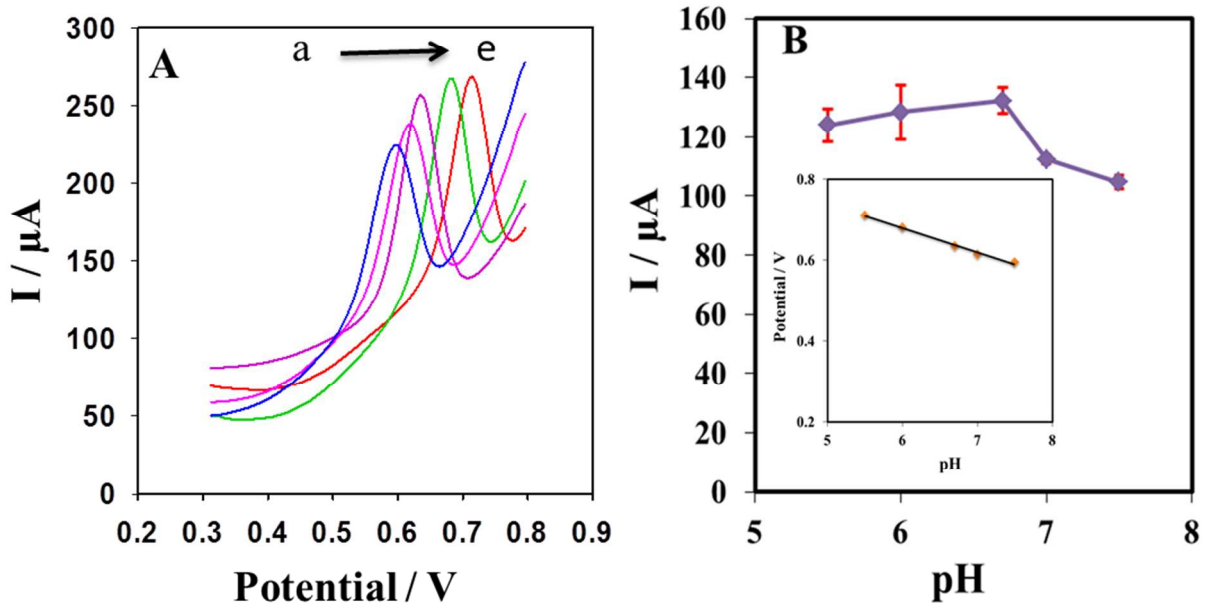

Fig. 6 (A) Square wave voltammograms in a 50 µM L-tyrosine 0.1 M L^{-1} PBS solution at various pH values (a) 7.5 pH, (b) 7.0 pH, (c) 6.7 pH, (d) 6.0 pH, (e) 5.5 at GR-modified GPE. (B) Graphical representation of the peak current vs. pH. Inset: Relationship between the pH and the oxidation peak potential.

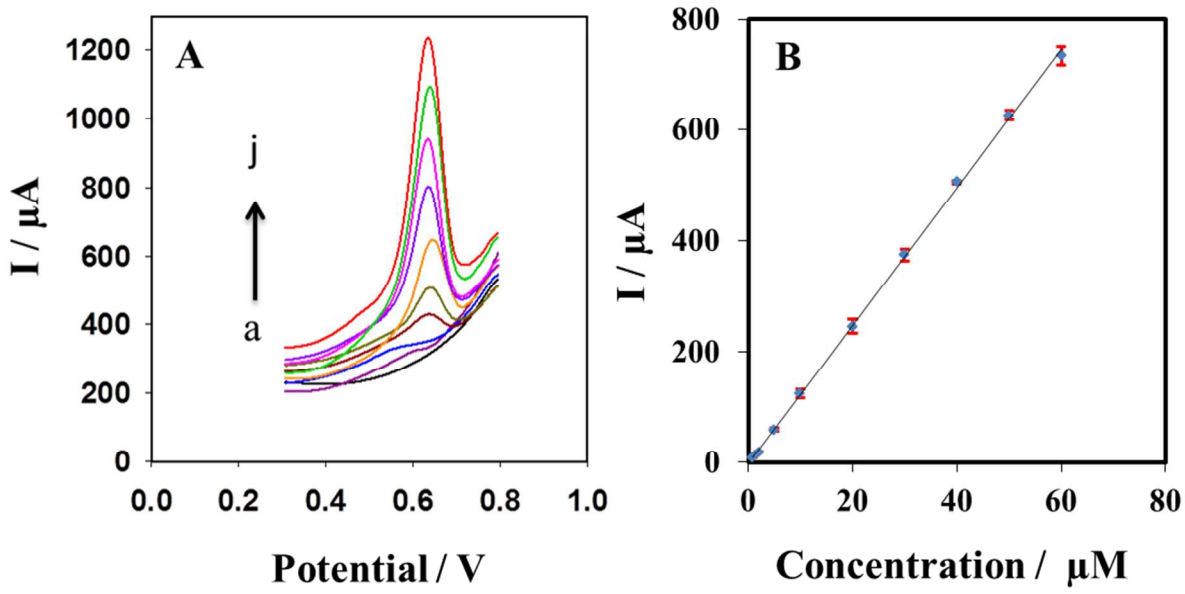

Fig. 7 (A) Square wave voltammograms in PBS buffer (0.1 M, pH 6.7) at various concentrations of tyrosine: (a) 0 µM, (b) 0.8 µM, (c) 2 µM, (d) 5 µM, (e) 10 µM, (f) 20 µM, (g) 30 µM, (h) 40 µM, (i) 50 µM, (j) 60 µM. The graph (B) showed the linear relationship between I (µA) and the concentration (µM) of L-tyrosine (R^2 = 0.9995), with the error bars. The SWV parameters were: amplitude of 0.03 V, frequency of 50 Hz, and adsorption time of 210 s.

Graphical Abstract